NASA TM X-719

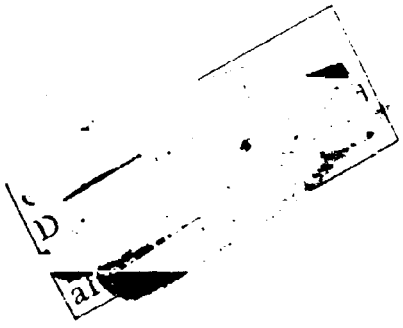

TECHNICAL MEMORANDUM
X-719

PERFORMANCE EVALUATION OF THREE-STAGE PROTOTYPE NERVA TURBINE DESIGNED FOR BLADE-JET SPEED RATIO OF 0.107

By Harold E. Rohlik and Milton G. Kofskey

Lewis Research Center
Cleveland, Ohio

NATIONAL AERONAUTICS AND SPACE ADMINISTRATION
WASHINGTON

January 1963

[redacted]

NATIONAL AERONAUTICS AND SPACE ADMINISTRATION

TECHNICAL MEMORANDUM X-719

PERFORMANCE EVALUATION OF THREE-STAGE PROTOTYPE NERVA TURBINE DESIGNED FOR BLADE-JET SPEED RATIO OF 0.107*

By Harold E. Rohlik and Milton G. Kofskey

SUMMARY

Performance characteristics of the NERVA turbine were investigated experimentally in cold nitrogen. At design blade-jet speed ratio the total-to-static efficiency was 0.45. Examination of design characteristics and experimental performance indicated that performance could be improved appreciably through redesign of the blading to obtain optimum solidities and blade shapes and thereby minimize viscous losses.

INTRODUCTION

The turbine research program at the NASA Lewis Research Center includes the study of turbines for various rocket propellant pump-drive applications. One type of turbine of considerable interest is that for a hydrogen-propelled rocket with a nuclear-reactor heat source. Analyses of turbines for this application show that they operate at low blade-jet speed ratios (around 0.10) because of the high energy content of the hot hydrogen relative to the blade speed, which is limited by conditions of temperature and stress. Studies such as that reported in reference 1 indicate that multistaging is required to obtain high turbine efficiency and, consequently, to minimize the turbine flow rate and the associated loss in effective specific impulse.

As part of this program an experimental investigation was undertaken to determine performance characteristics of a prototype turbine designed for the NERVA (Nuclear Engine for Rocket Vehicle Application) program. The NERVA turbine, 10.92 inches in mean diameter, was designed for a pressure ratio of 10, a blade-jet speed ratio of 0.107, and a total-to-static efficiency of 0.43. It was made available to NASA for performance evaluation by the Aerojet-General Corporation. The experimental tests

*Title, Unclassified.

[redacted]

were made with cold nitrogen and included one-, two-, and three-stage operation over ranges of speed and pressure ratio.

This report presents the details of the performance measurements, a comparison of efficiency characteristics with those of two other turbines designed for similar operating requirements, and recommendations for improving the performance of the NERVA turbine.

SYMBOLS

c_p specific heat at constant pressure, Btu/(lb)(^oR)

D_p pressure-surface diffusion parameter, $1 - \frac{V_{s,min}}{V_e}$

D_s suction-surface diffusion parameter, $1 - \frac{V_e}{V_{s,max}}$

D_{tot} sum of suction- and pressure-surface diffusion parameters, $D_p + D_s$

g acceleration due to gravity, 32.17 ft/sec^2

Δh turbine specific work, Btu/lb

J mechanical equivalent of heat, 778.2 ft-lb/Btu

N rotative speed, rpm

p absolute pressure, lb/sq ft

R gas constant, 55.16 in nitrogen, ft-lb/(lb)(^oR)

T absolute temperature, ^oR

U blade velocity, ft/sec

V absolute gas velocity, ft/sec

V_{cr} critical velocity, $\sqrt{\frac{2\gamma g R T'}{\gamma + 1}}$, ft/sec

V_j ideal jet speed corresponding to total- to static-pressure ratio across turbine, $\sqrt{2gJc_pT_i'\left[1 - \left(\frac{p_e}{p_i'}\right)^{\frac{\gamma-1}{\gamma}}\right]}$, ft/sec

w weight flow, lb/sec

γ ratio of specific heats

δ ratio of inlet total pressure to NACA standard sea-level pressure, $p_i'/2116.2$

ϵ function of γ used in relative weight flow to that using inlet conditions at NACA standard sea-level atmosphere, $\frac{0.740}{\gamma}\left(\frac{\gamma + 1}{2}\right)^{\frac{\gamma}{\gamma-1}}$

η_s turbine efficiency based on total- to static-pressure ratio across turbine and turbine shaft work

θ_{cr} squared ratio of turbine-inlet critical velocity to that of NACA standard sea-level atmosphere, $\left(\frac{V_{cr,i}}{1019}\right)^2$

ν blade-jet speed ratio, U_m/V_j

Γ torque, ft-lb

Subscripts:

e exit

i inlet

m mean radius

max maximum

min minimum

s surface

Superscript:

' absolute total state

TURBINE DESCRIPTION

Overall Requirements

The three-stage NERVA turbine power and speed requirements resulted from the following pump characteristics:

Rotative speed, N, rpm	21,800
Weight flow, w, lb/sec	73.5
Pressure rise, lb/sq in.	800
Pump efficiency	0.75

The overall turbine design requirements are presented in the following table:

Parameter	Hydrogen	NACA standard air conditions
Weight flow, w, lb/sec	4	0.6607
Specific work, Δh, Btu/lb	816.3	25.86
Rotative speed, N, rpm	21,800	3880
Inlet temperature, T_i, $^{\circ}R$	1140	518.7
Inlet pressure, p_i, lb/sq ft abs	72,000	2116
Pressure ratio, p_i'/p_e	10	10
Static efficiency, η_s	0.43	0.43
Blade-jet speed ratio, ν	0.107	0.107

Overall Geometry

Figure 1 shows a cross section of the NERVA turbine. The blade rows have a constant mean diameter with annular area variation to obtain the desired axial velocities through the turbine. Figure 1 also shows that large axial clearances between blade rows were used through the turbine. The average axial clearance was 0.230 inch.

In order to minimize leakage between stages, labyrinth shaft seals were used on the second- and third-stage stators. The seals were located on a 3-inch diameter, and the clearance between the seal and the rotor hub was 0.005 inch. Figure 2 presents schematics of the other four configurations investigated and shows the location of spacers used in place of the other stage parts.

Stator Description

Blade profiles and passages are shown in figure 3. The figure shows that the first-stage stator profile was essentially a flat plate. Second- and third-stage stators were of airfoil-type profiles of straight back design.

Free-stream turning through the stators was approximately 75°, 137°, and 126° for the first, second, and third stages, respectively. The design resulted in 56, 80, and 80 stator blades with solidities of 1.68, 2.10, and 2.15 based on actual blade chord for the first, second, and third stages, respectively. Stator-blade heights were 0.316 and 0.487 inch for the first and second stages and 0.884 inch at the exit of the third stage. The aspect ratios were 0.307, 0.541, and 0.867 (based on average blade height) for the first, second, and third stages, respectively.

Rotor Description

Rotor-blade profiles and passages are also shown in figure 3. The rotor-blade passages were of circular-arc design, and the rotors had 103, 131, and 113 blades; this resulted in comparatively low solidities of 0.90, 1.34, and 1.32 for the first, second, and third stages, respectively. Blade heights were 0.430, 0.618, and 0.967 inch, and free-stream turning was 144°, 133°, and 125° for the first, second, and third stages, respectively. Aspect ratios were 1.43, 1.76, and 2.42, and the radial tip clearances were 0.038, 0.054, and 0.050 inch, which amount to 8.8, 8.7, and 5.2 percent of the blade height. A photograph of the three-stage rotor is shown in figure 4.

APPARATUS AND INSTRUMENTATION

The test facility used in the experimental investigation was the same as that described in reference 2 and consisted of an inlet ducting system with pressure controls, the turbine test section, and exit ducting that exhausted to the atmosphere through a pressure control system. Power was absorbed by an eddy-current cradled dynamometer that also served as a speed control. Figure 5 shows the arrangement of these parts in the test building.

Actual specific-work output was computed from weight flow, torque, and speed. The weight flow was measured with a calibrated ASME flat-plate orifice, and turbine output torque was measured with a commercial self-balancing torque cell. Turbine-inlet measurements of pressure and temperature were taken in the annulus upstream of the first-stage stator inlet (figs. 1 and 2). Turbine-exit static pressures were measured in the annulus downstream of the rotor outlet (figs. 1 and 2).

EXPERIMENTAL PROCEDURE

Test data were recorded on magnetic tape during steady-state operation over a range of pressure ratios and rotative speeds. In order to

maintain turbine torque adequate for speed control, two modes of operation were used. For the high-pressure-ratio range, the exhaust pressure was held constant at a nominal value of 15 pounds per square inch absolute, and the inlet pressure was varied from 100 to 150 pounds per square inch absolute. For the low-pressure-ratio range, the inlet pressure was held nominally constant at 100 pounds per square inch absolute, and the exhaust pressure was varied from 16 to 70 pounds per square inch absolute. The turbine-inlet temperature was nominally 0° F, but the actual temperature depended on the ambient temperature and expansion within the gas storage vessels during a run. Rotative speed was varied from 20 to 120 percent of design speed in increments of approximately 20 percent.

Six test runs were made to obtain the data presented for the five configurations investigated. In each run a series of pressure ratios were held nominally constant while turbine speed was varied over the desired range. The five configurations were:

(1) First, second, and third stages

(2) First and second stages

(3) First stage

(4) Second stage

(5) Third stage

RESULTS AND DISCUSSION

The NERVA turbine performance, as determined in cold nitrogen, is presented as curves of efficiency and specific performance parameters reduced to standard air at the inlet. This performance is compared with that of reference turbines of similar nature.

Overall Efficiency

Figure 6 shows the variation of static efficiency with blade-jet speed ratio for the first stage and first and second stages and for the complete three-stage turbine. The points plotted include all pressure-ratio - speed combinations tested. The three-stage efficiency was 0.45 at the blade-jet speed ratio corresponding to the speed and overall pressure ratio specified for design operation. This is 0.02 higher than the efficiency listed for design operation. The differences in level among the three curves result from three factors: (1) The first of these is the difference in design blade-jet speed ratios. At any three-stage operating point, the corresponding blade-jet speed ratios of the individual stages in the turbine are considerably higher than the overall

blade-jet speed ratio because of the lower stage pressure ratios. For a given efficiency level, therefore, increasing the number of stages simply moves the overall operating point to lower values of blade-jet speed ratio. (2) The kinetic energy of fluid leaving the first and second stages is available to the following stator and is not completely lost as in the calculation of static efficiency. (3) The effect of reheat elevates the overall efficiency over that of the individual stages. The effect of staging on velocity diagrams and efficiency characteristics is discussed at length in reference 1. Other factors that may have contributed to differences among the stages are the solidities, the aspect ratios, the tip clearances, and the ratios of flow area to wetted area, which were not constant for the three stages.

Weight Flow

Figure 7 shows the variation in weight flow with pressure ratio and speed for the three-stage turbine. The turbine was choked for all pressure ratios above 3 at a value of 0.66 pound per second, the same value specified for design operation. Choking weight-flow values showed no effect of speed, which indicates that the first stator was choked.

Turbine Work and Torque

Equivalent specific work is shown in figure 8 as a function of speed for various pressure ratios. Limitations in the test-rig ducting prevented operation at the design pressure ratio of 10. The maximum pressure ratio attainable was 9.6, as noted in figure 8. The curves (fig. 8) were cross-plotted for figure 9 in order to extrapolate pressure ratio. The design speed line of figure 9 shows that the design operation specific work of 25.86 Btu per pound was reached at a pressure ratio of 8.8. The high-constant-speed lines have a slight positive slope at a pressure ratio of 10, which indicates that limiting loading had not been reached.

Figure 10 shows equivalent torque as a function of speed for each pressure ratio tested. The zero-speed torque values obtained with the dynamometer rotor bolted to the stator are shown in figure 11. The curves of figure 10 are typical of single and multistage turbines in that they are nearly linear with speed. The margin between design-speed torque and zero-speed torque is relatively small (i.e., about 40 percent of design torque), while the runaway speed is more than twice the design speed. Extrapolating the 9.6-pressure-ratio curve to zero torque indicates that, if the turbine load were removed, the turbine could accelerate to more than three times design rotative speed.

Single-Stage Performance

Performance of each of the stages was measured with the same instrumentation used for overall performance determination and spacers in place of other stage parts. Measured performance of the second and third stages, therefore, included appreciable losses between the inlet pipe (where inlet pressure was measured) and the stator inlet. The magnitudes of these losses were determined at design speed and overall pressure ratio by iteration, that is, by estimating the total-pressure loss, adjusting performance to correspond to the loss, and then comparing overall pressure ratio, equivalent flows, and total work with the measured values. Losses determined in this manner were 18 percent of inlet pressure from the turbine inlet to the second stator and 46 percent from the turbine inlet to the third stator. Figure 12 shows the curves of stage static efficiency as functions of the stage blade-jet speed ratio adjusted for these losses. The level of loss was experimentally verified in a brief test with a total-pressure probe located just upstream of the third stator. In this test a high-recovery shielded total-pressure probe was positioned at midblade height and rotated for maximum pressure reading. At the optimum probe angle the measured pressure showed a loss near that calculated for the second between the inlet measuring station and the third stator. Figure 12 is, therefore, believed to be an accurate representation of the individual stage performance. No data points are shown because of the adjusted levels resulting from the calculated losses. The symbols shown represent the stage operating points with the complete turbine operating at design speed and overall pressure ratio. The individual stages operate at nearly the same blade-jet speed ratio (viz., 0.16 to 0.18) and at comparable efficiencies. At design operation the first-stage efficiency is lowest at 0.35, the second-stage efficiency highest at 0.39, and the third intermediate at 0.36.

Performance Comparison

The efficiency characteristics were compared with those of two other turbines designed for low blade-jet speed ratios. These turbines were an eight-stage unit for a hydrogen-propelled-nuclear-reactor rocket and a three-stage turbine designed for a hydrogen-oxygen chemical rocket. The design blade-jet speed ratios were 0.110 and 0.156, respectively. Both were designed and tested in cold gas by NASA.

The design application and parameters for the NASA turbines are fully described in references 3 to 5. The design blade-jet speed ratios for the reference turbines were determined by the required work and speed as well as stress and temperature considerations. The numbers of stages resulted from optimization studies, which considered the effects of turbine weight and turbine flow on the gross- to pay-weight ratio of the rocket for a given mission. In each of the optimization studies the

significance of turbine efficiency, and hence required turbine flow, led to the selection of enough turbine stages to result in stage blade-jet speed ratios of 0.25 to 0.30 and overall efficiencies near 0.65.

The limitation to three stages for the subject turbine was influenced by reliability considerations and resulted largely from the decision to use a cantilever turbine rotor mount rather than a system of bearings both upstream and downstream of the turbine. This necessarily limited the turbine to lower stage blade-jet speed ratios and lower efficiencies.

Figure 13 shows experimentally determined static efficiency as functions of blade-jet speed ratio for all three turbines. The curves of figure 13 show three appreciably different levels in the region of the design blade-jet speed ratio. At comparable stage blade-jet speed ratios, the difference in efficiency between the NASA three-stage and eight-stage turbines is largely the result of stage number. The difference in stage number results simply in the occurrence of peak overall efficiency at different overall blade-jet speed ratios.

The difference in efficiency between the two three-stage turbines results primarily from the difference in design method. The NASA turbine design included calculation of stator- and rotor-blade surface velocities in order to keep diffusion and, consequently, boundary layer losses within reasonable limits. The total diffusion D_{tot}, which represents the sum of the blade surface velocity decelerations, was limited to 0.4 in the stators and 0.6 in the rotors. The relation between total diffusion and blade row loss is described in reference 6. The blade solidities resulting from these design controls were 1.8 to 2.3 in the rotors, compared with 0.9 to 1.3 in the subject turbine. Reference 7 describes the effects of changes in turbine geometry on turbomachine viscous loss and includes curves of optimum solidity and aspect ratio. The curves indicate optimum solidities of 1.6, 1.9, and 2.0 for the NERVA rotors.

Reference 6 relates boundary-layer characteristics to blade-row losses. The analysis method described indicates that optimum rotor solidities with the same aspect ratios would reduce boundary-layer losses in the subject turbine by 45, 28, and 30 percent in the first, second, and third rotors, respectively. Examination of kinetic energy in the rotors shows that reduction of rotor losses by these amounts would increase turbine efficiency by approximately 0.035, a gain of 8 percent.

Examination of the turbine geometry also showed that excessive losses might be incurred in the rotor-blade tip region. The rotor tip clearances noted previously were 8.8, 8.7, and 5.2 percent of blade height. Calculation of clearance required for differential thermal expansion, stress growth, and machine tolerance showed that these clearances

could safely be reduced by 50 percent. Reference 8 presents the effect of rotor tip clearance on performance of a single-stage turbine similar in size and blade-jet speed ratio. In that investigation turbine work decreased linearly with increase in tip clearance in the 3- to 10-percent range. The rate of decrease was 0.9 percent in turbine work for 1.0 percent in blade height for the type of tip clearance in the NERVA turbine. This indicates a gain of 0.015 in turbine efficiency for a reduction of 50 percent in tip clearance. The large axial clearances might also contribute to the tip loss by permitting the free-stream flow near the stator tip to expand into the larger annular areas and partially bypass the rotor-blade tips.

Figure 14 shows a performance comparison for the first stages of the turbines previously compared. This figure provides a common basis for comparison of the three turbines and illustrates appreciable differences in efficiency levels at the design blade-jet speed ratio of the NERVA turbine. The difference results from the NERVA stator geometry selected (a cascade of straight vanes that required the flow to accelerate from the inlet plenum to near-sonic velocity without guidance during the turning and acceleration), the larger tip clearances, and the large deviations from optimum rotor-blade solidities. The two NASA turbines were designed for much higher stage blade-jet speed ratios and, consequently, have some incidence losses at the design blade-jet speed ratio of the NERVA turbine. Design for the same blade-jet speed ratio would, therefore, result in a somewhat larger difference in efficiency.

Significance of Turbine Performance

The performance of a rocket turbopump turbine affects rocket performance through the required turbine flow, which reduces rocket nozzle flow and, therefore, effective specific impulse. The subject turbine requires 5.4 percent of the pump flow to provide power to drive the pump. The high level of this value results from the low inlet temperature and low efficiency of the turbine. Since turbine flow rate varies inversely with each of these quantities, increasing the inlet temperature to 1860° R (which would require a modification in the rocket flow system) and increasing the turbine efficiency to 0.65 (which would require additional stages) would reduce turbine flow to 2.3 percent of pump flow. The significance of this increase in temperature and efficiency in regard to payload capacity is demonstrated in reference 9, which shows the ratio of gross weight to payload as a function of bleed rate for given values of mission and structural parameters. The bleed rates of 5.4 and 2.3 at representative structural parameters for a single-stage satellite-launch vehicle result in gross- to payload-weight ratios of 25.3 and 22.07, respectively, when the turbine exhaust specific impulse is 50 percent of the rocket nozzle specific impulse. The turbine temperature and efficiency increases would, therefore, provide a 15 percent improvement in

payload capability. If the turbine exhaust provides zero thrust recovery, the increase is substantially larger, with gross- to payload-weight ratios of 37.9 and 24.9 for bleed rates of 5.4 and 2.3, respectively. The payload capability would therefore increase 52 percent.

The limits defined for the NERVA turbine design included the inlet temperature of 1140° R and the cantilever turbine mount with three turbine stages. Improvement in turbine efficiency within these limits must, therefore, come from improvement in blade design. The improvement in efficiency expected from improved design, can be estimated from figure 13, which shows efficiencies of 0.516 and 0.446 for the two three-stage turbines at the NERVA turbine design blade-jet speed ratio of 0.107. Examination of the blade geometry and reference material indicates that a gain of 5 to 7 points in efficiency could be expected by replacing the first stator with carefully designed stator blades, reducing tip clearance by 50 percent, and increasing the rotor solidities to the optimum values listed previously. An improvement of 0.05 in efficiency would reduce the turbine flow by 10 percent. The calculated gains in payload capability for this reduction in turbine flow would be 7 percent with a 50-percent turbine-exhaust thrust-recovery system and 11 percent with a zero-thrust-recovery system.

CONCLUDING REMARKS

The experimental investigation of the NERVA turbine showed a design-point efficiency of 0.45. This efficiency and the specified inlet temperature result in a turbine flow rate of 5.4 percent of the total pump flow. The design selections of three stages and an inlet temperature of 1140° R were based on reactor plumbing and reliability considerations, although they place a severe penalty on rocket performance. An additional penalty on rocket performance is incurred by turbine losses due to deviations from optimum geometry. Increasing the number of turbine stages, improving blade design, and raising the turbine-inlet temperature to the limit set by turbine materials could reduce the turbine flow rate by more than 50 percent.

The larger penalties are inevitable with the limitations specified for turbine-inlet temperature and stage number. The deviations from optimum blade geometry, however, are not, and could be rather easily remedied with new aerodynamic design of the blade rows and reduced tip clearances.

Lewis Research Center
National Aeronautics and Space Administration
Cleveland, Ohio, August 9, 1962

REFERENCES

1. Stewart, Warner L.: Analytical Investigation of Multistage-Turbine Efficiency Characteristics in Terms of Work and Speed Requirements. NACA RM E57K22b, 1958.

2. Wong, Robert Y., and Darmstadt, David L.: Comparison of Experimentally Obtained Performance of Two Single-Stage Turbines with Design Ratios of Blade to Jet Speed of 0.191 and 0.262 Operated in Hydrogen and in Nitrogen. NASA TM X-415, 1961.

3. Kofskey, Milton G.: Cold-Air Performance Evaluation of a Three-Stage Turbine Having a Blade-Jet Speed Ratio of 0.156 Designed for a 100,000-Pound-Thrust Hydrogen-Oxygen Rocket Turbopump Application. NASA TM X-477, 1961.

4. Rohlik, Harold E.: Investigation of Eight-Stage Bleed-Type Turbine for Hydrogen-Propelled Nuclear Rocket Applications. I - Design of Turbine and Experimental Performance of First Two Stages. NASA TM X-475, 1961.

5. Rohlik, Harold E.: Investigation of Eight-Stage Bleed-Type Turbine for Hydrogen-Propelled Nuclear Rocket Applications. II - Experimental Overall and Stage Group Performance Determined in Cold Nitrogen. NASA TM X-481, 1962.

6. Stewart, Warner L., Whitney, Warren J., and Wong, Robert Y.: A Study of Boundary Layer Characteristics of Turbomachine Blade Rows and Their Relation to Over-All Blade Loss. Paper 59-A-23, ASME, 1960.

7. Miser, James W., Stewart, Warner L., and Whitney, Warren J.: Analysis of Turbomachine Viscous Losses Affected by Changes in Blade Geometry. NACA RM E56F21, 1956.

8. Kofskey, Milton G.: Experimental Investigation of Three Tip-Clearance Configurations over a Range of Tip Clearance Using a Single-Stage Turbine of High Hub- to Tip-Radius Ratio. NASA TM X-472, 1961.

9. Rohlik, Harold E., and Crouse, James E.: Analytical Investigation of the Effect of Turbopump Design on Gross-Weight Characteristics of a Hydrogen-Propelled Nuclear Rocket. NASA MEMO 5-12-59E, 1959.

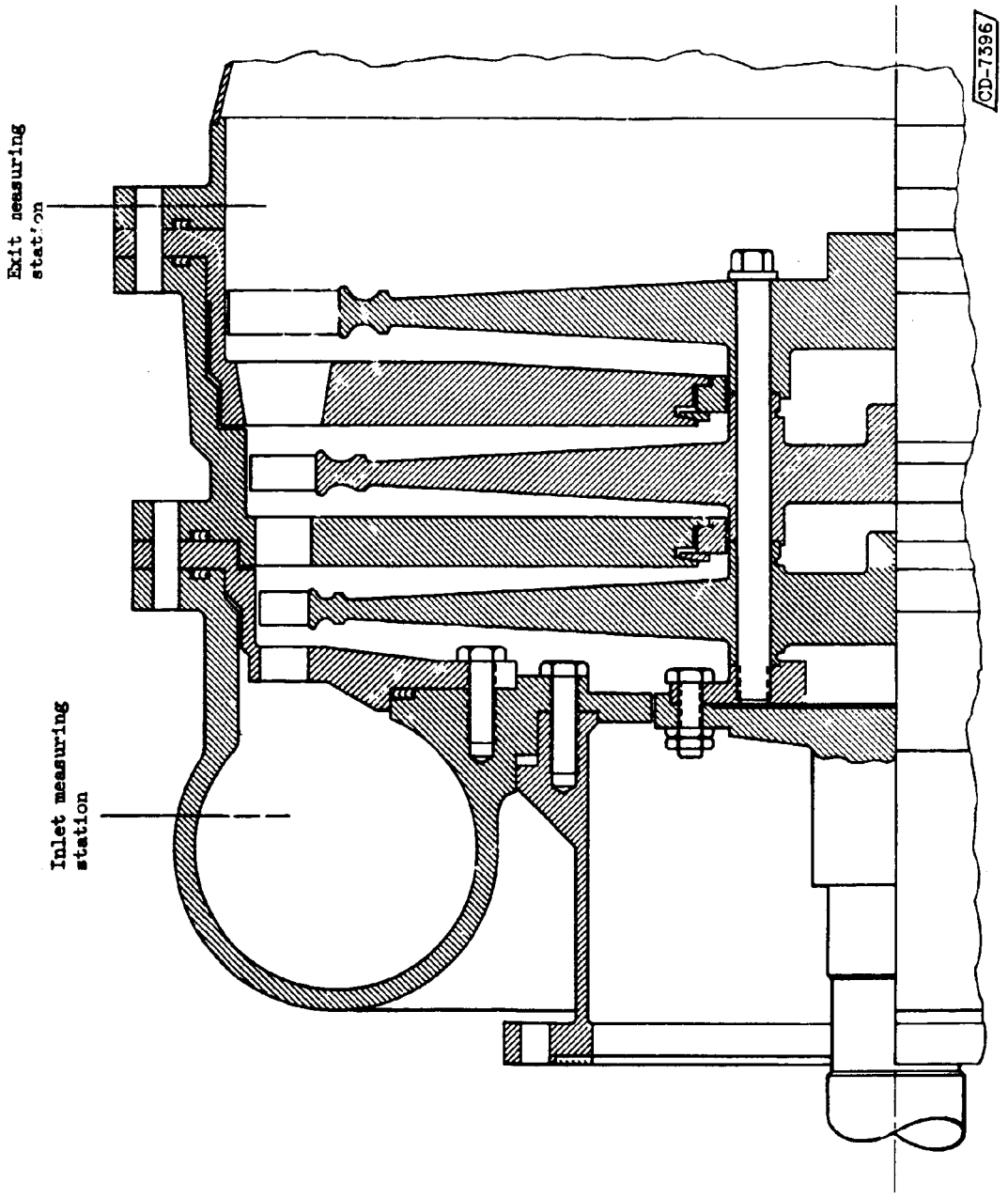

Figure 1. - Cross section of NERVA turbine.

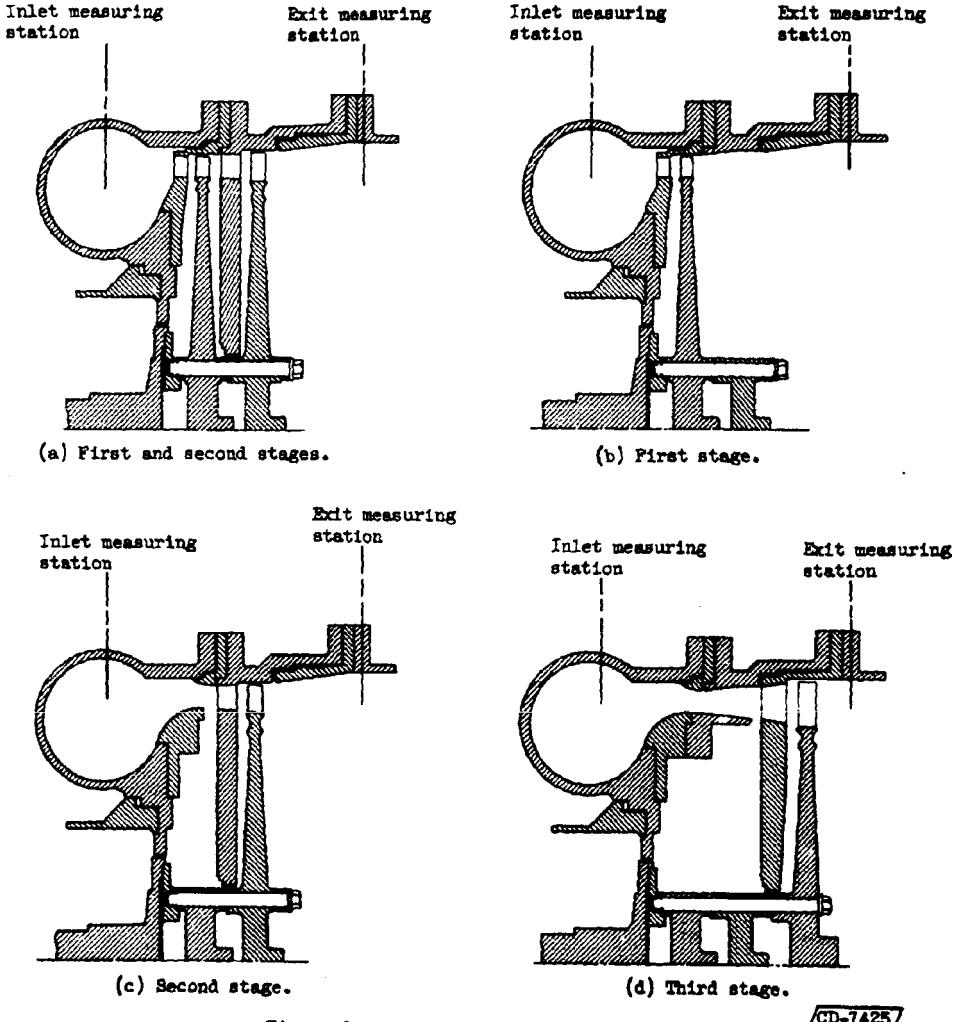

Figure 2. - Turbine components tested.

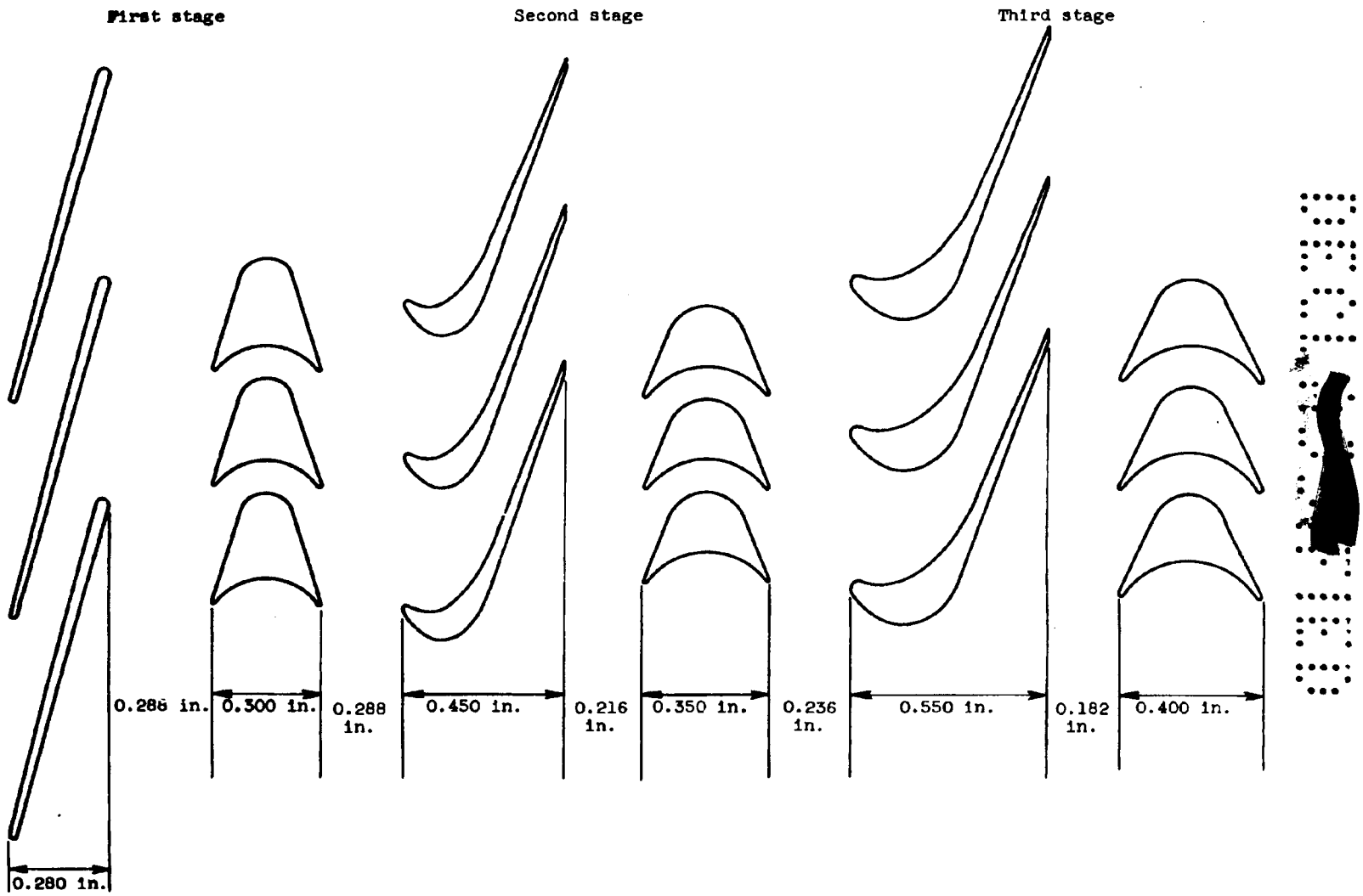

Figure 3. - Blade profiles and passages.

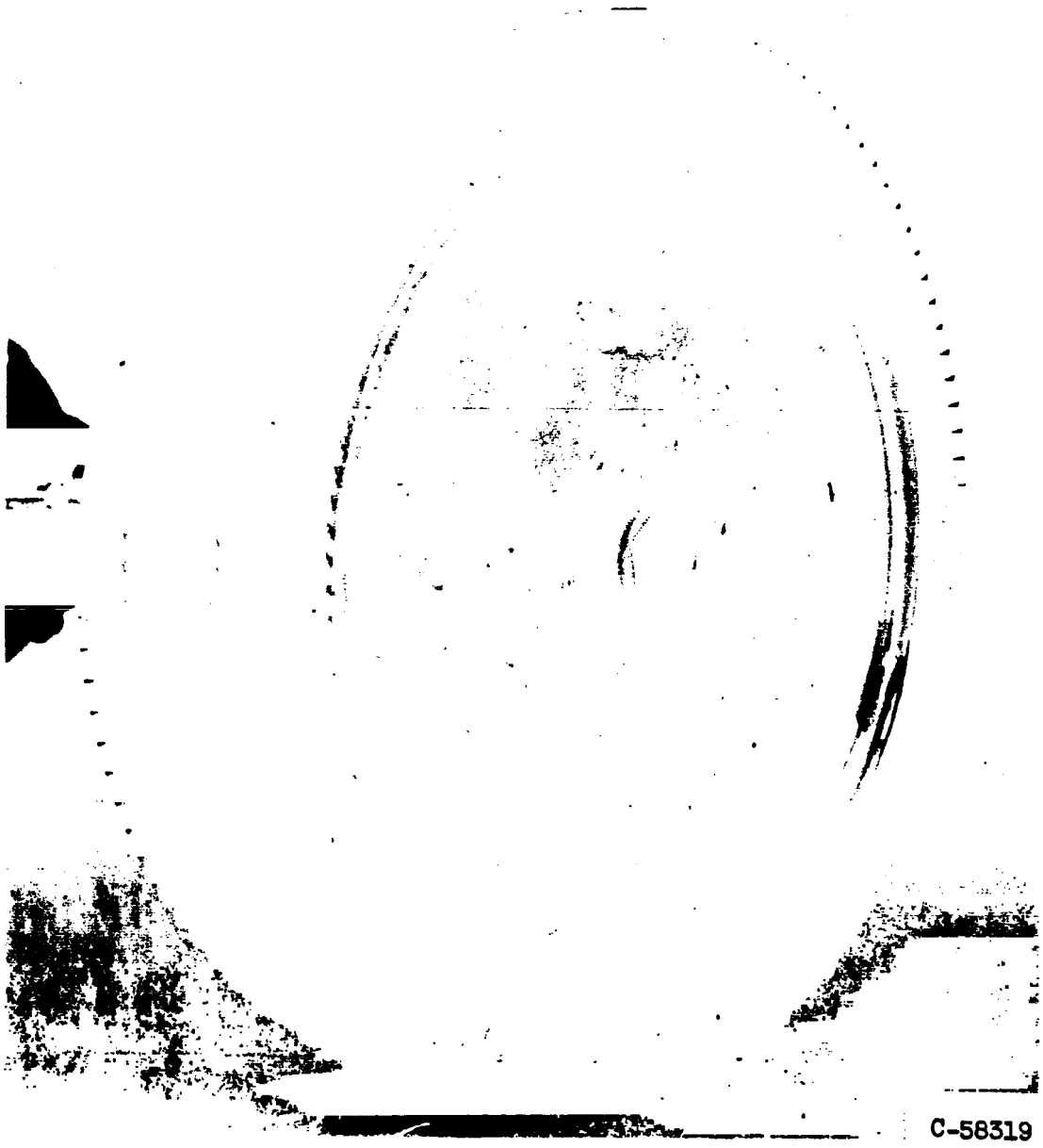

Figure 4. - NERVA turbine rotor

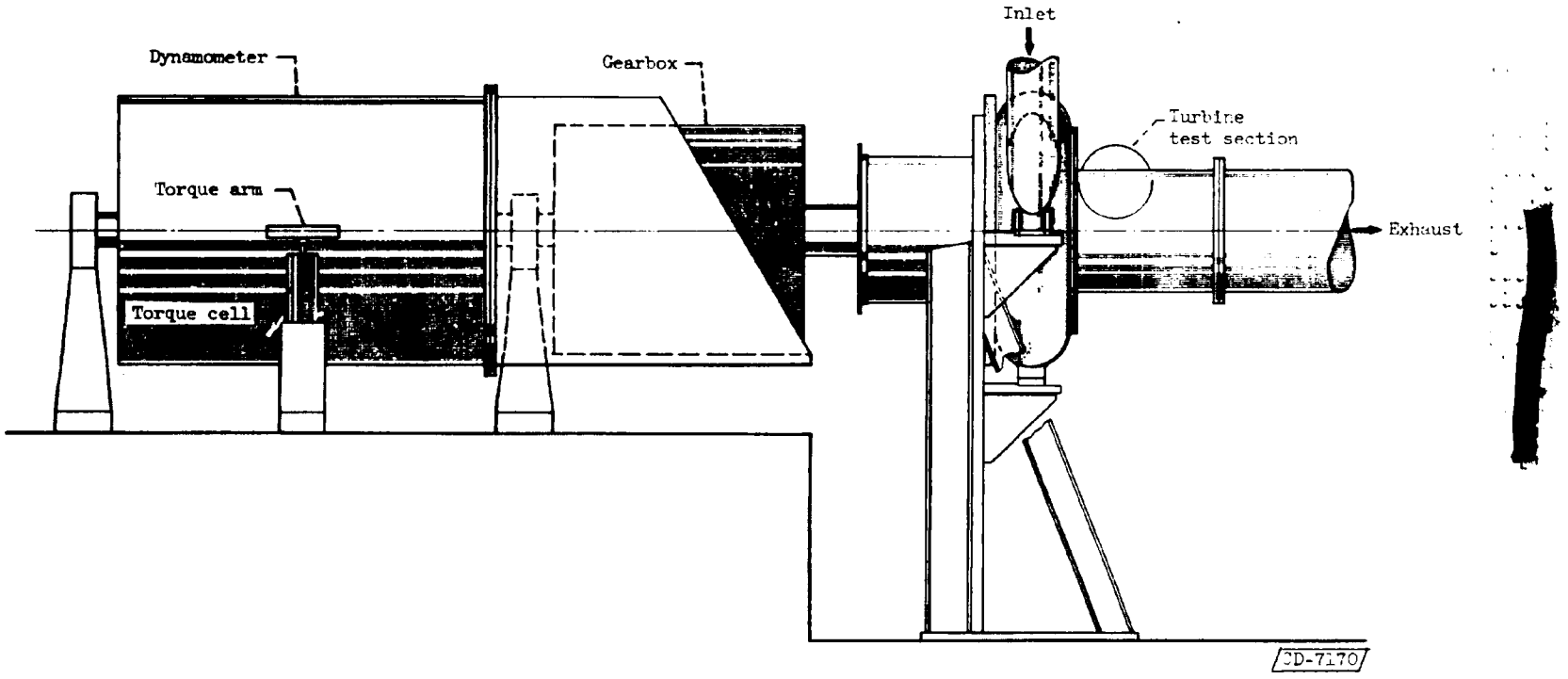

Figure 5. - Test equipment.

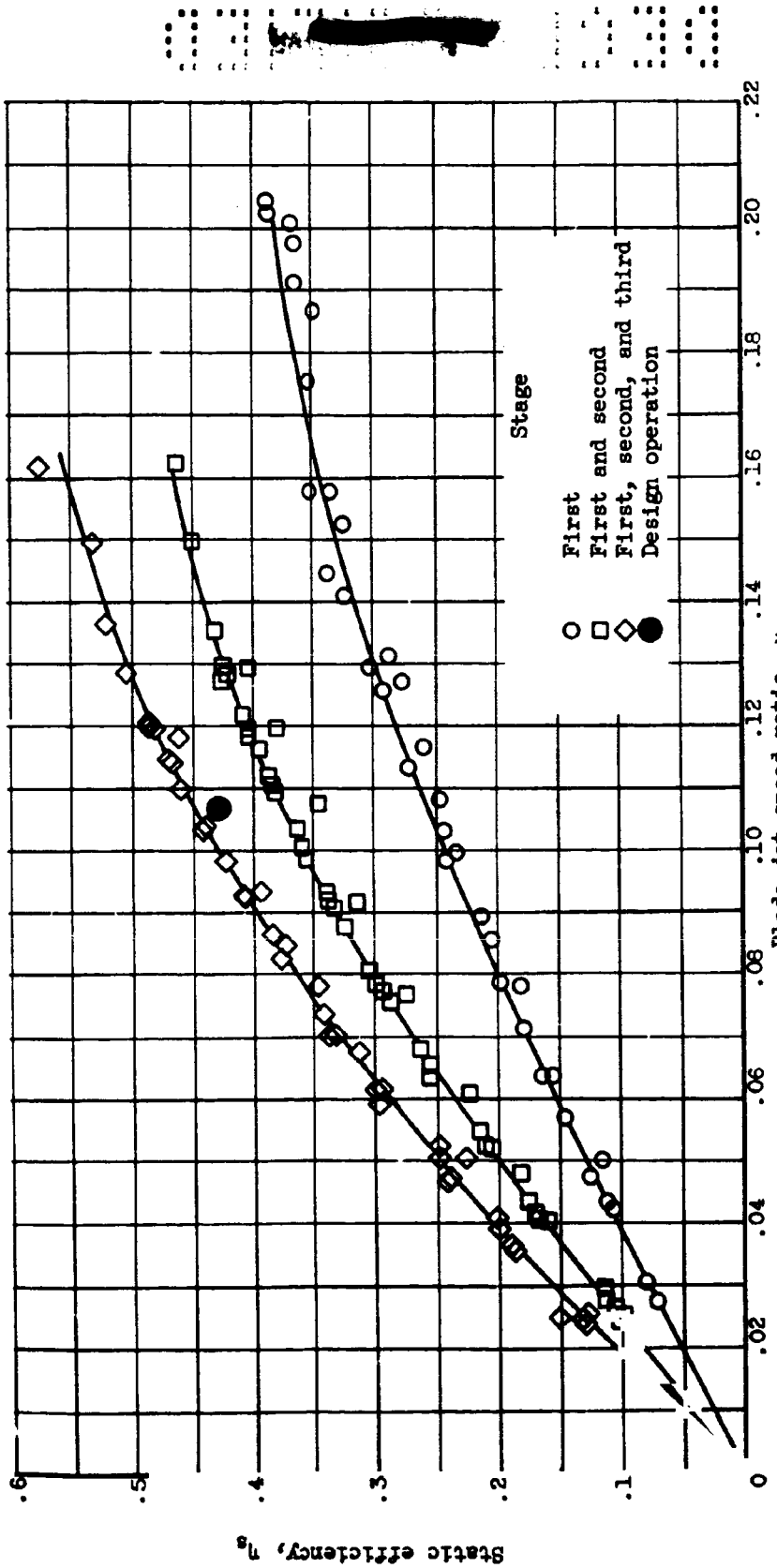

Figure 6. - Variation of static efficiency with blade-jet speed ratio.

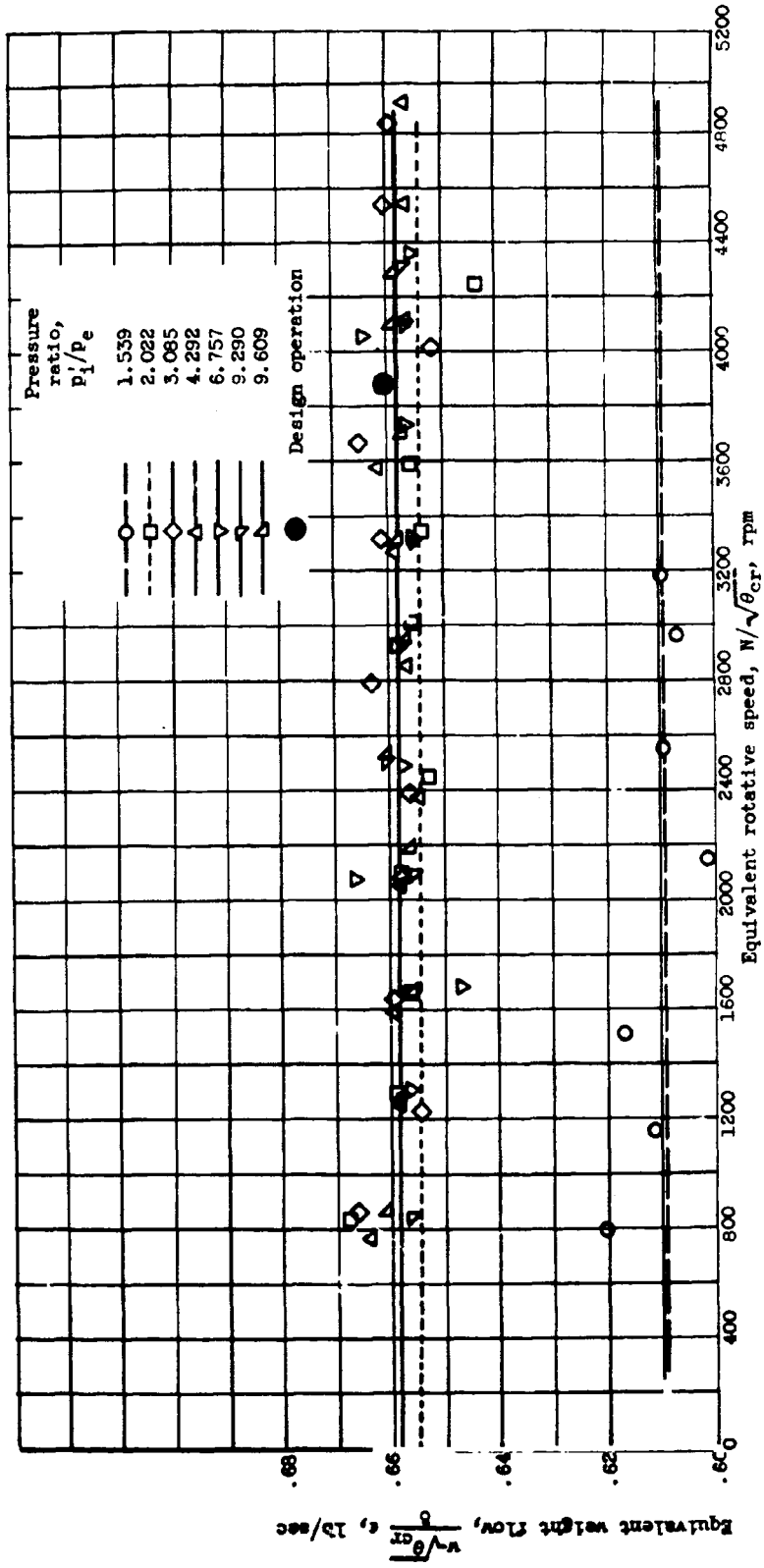

Figure 7. - Variation of weight flow with speed at various pressure ratios.

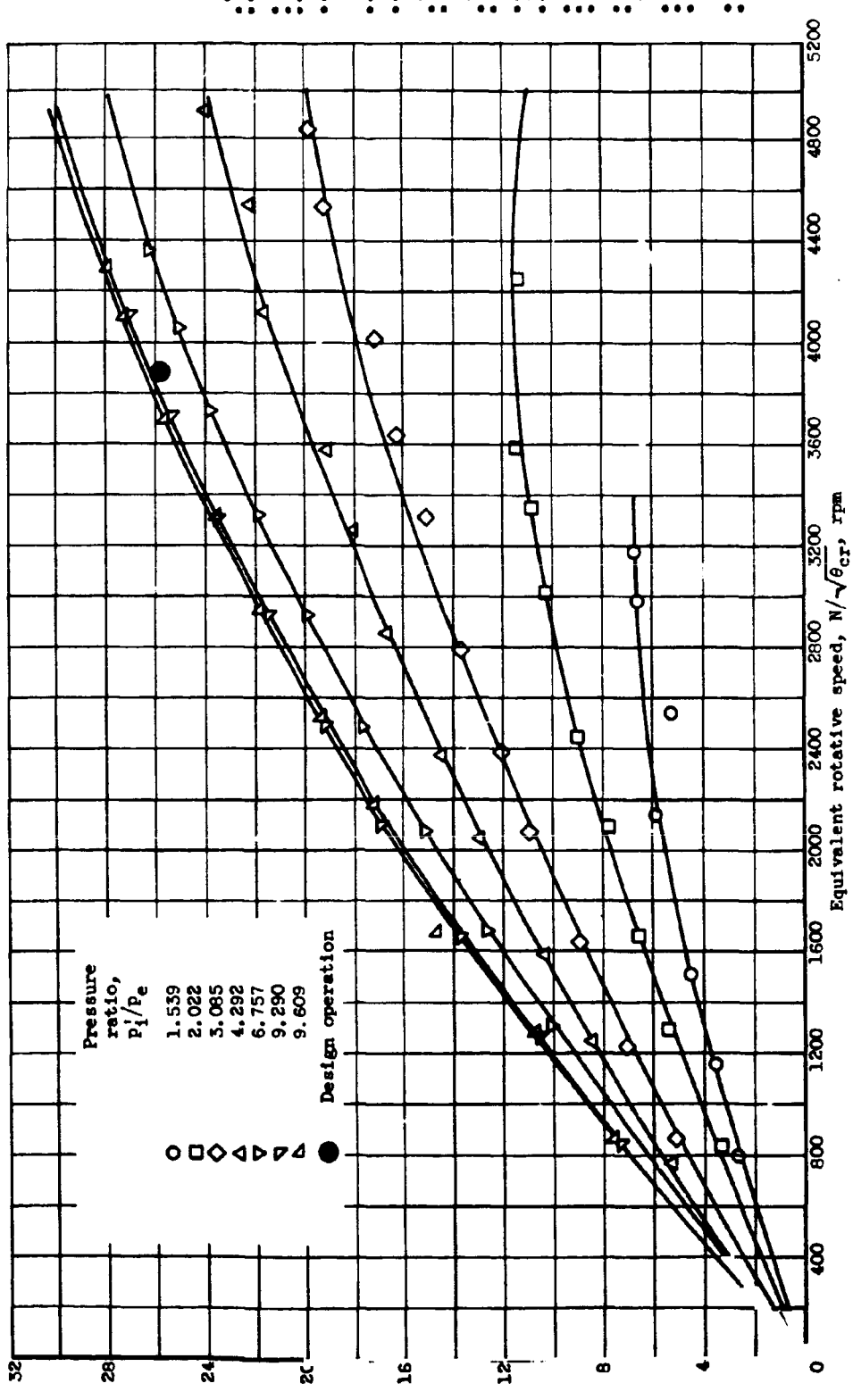

Figure 8. - Variation of specific work with speed at various pressure ratios.

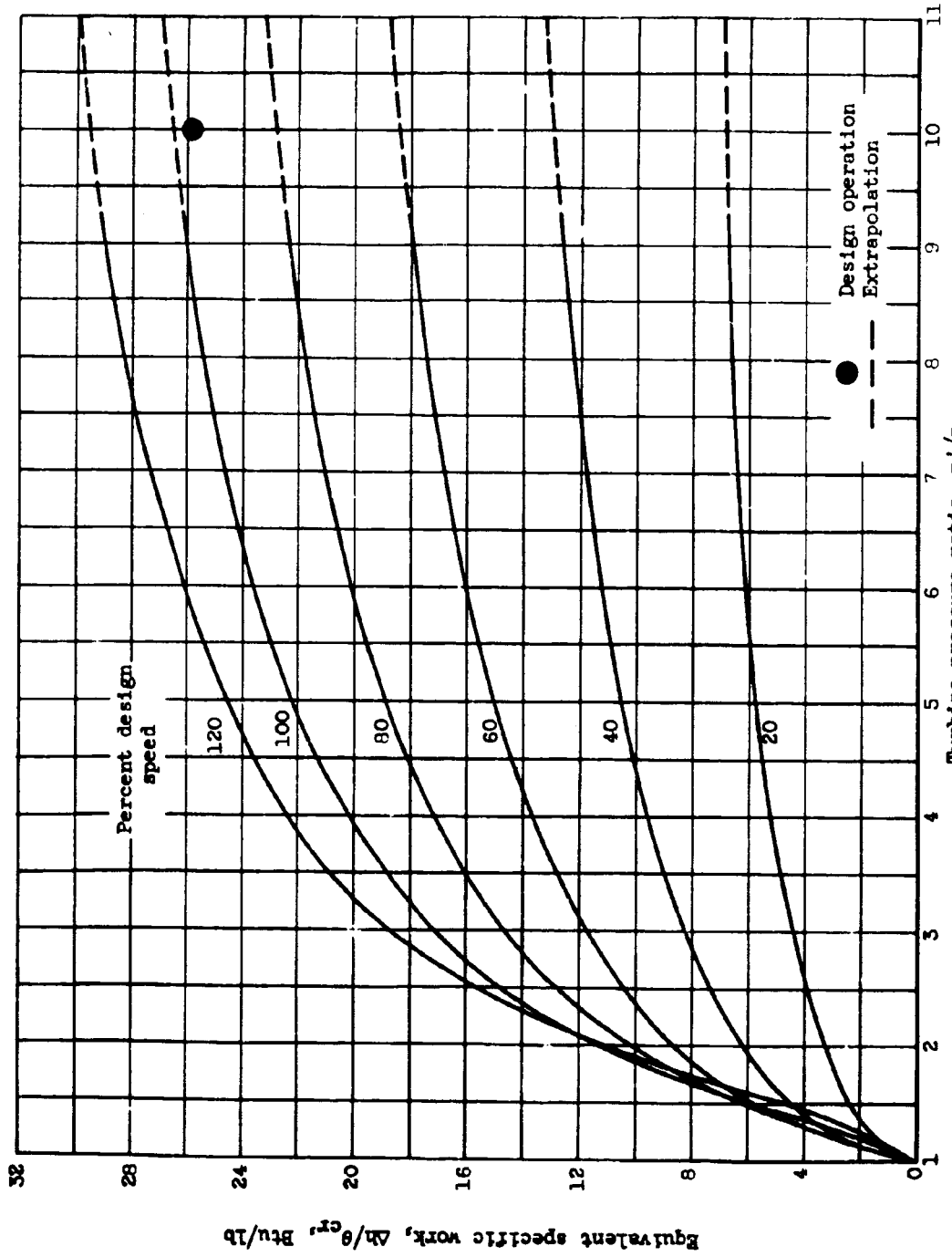

Figure 9. - Variation of specific work with pressure ratio at various speeds.

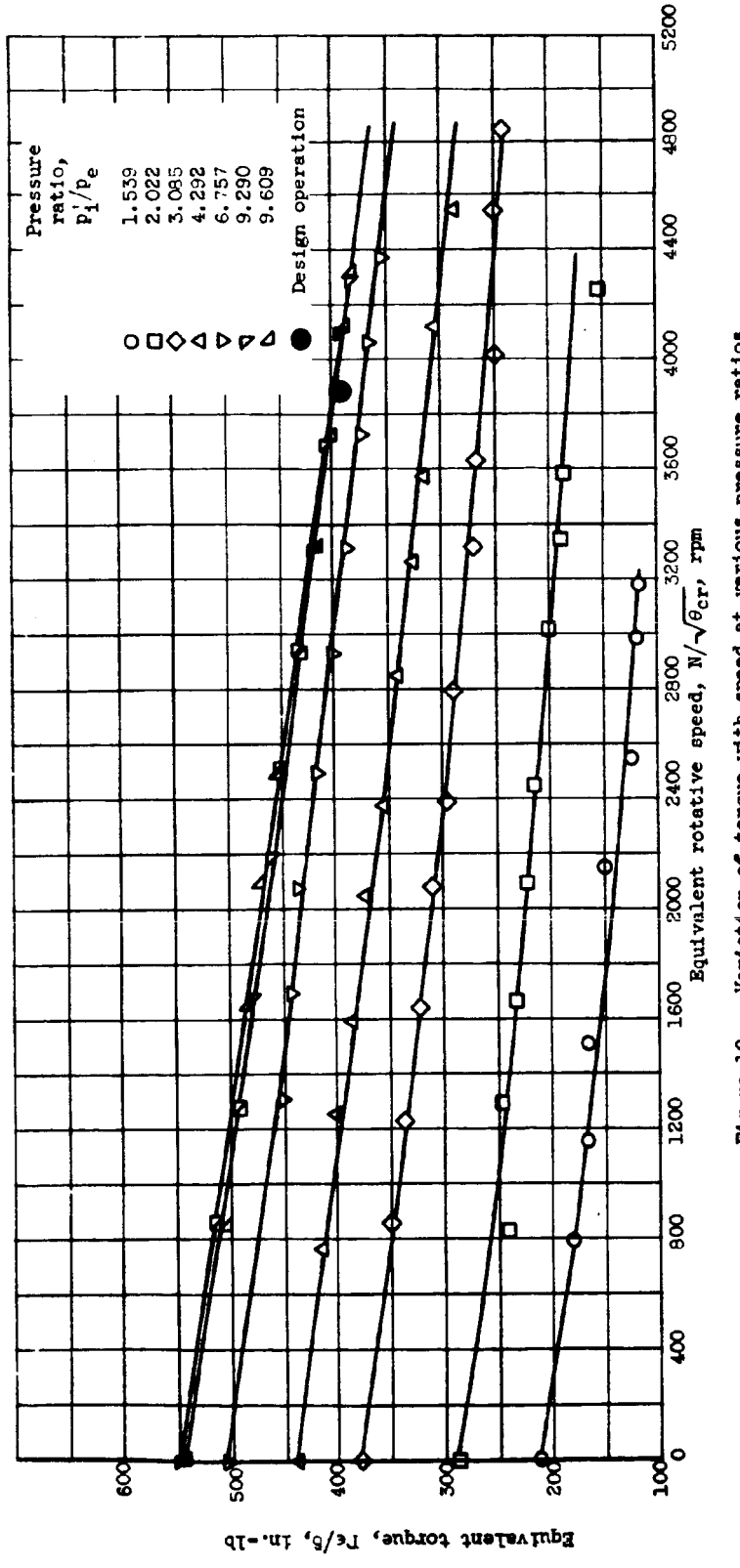

Figure 10. - Variation of torque with speed at various pressure ratios.

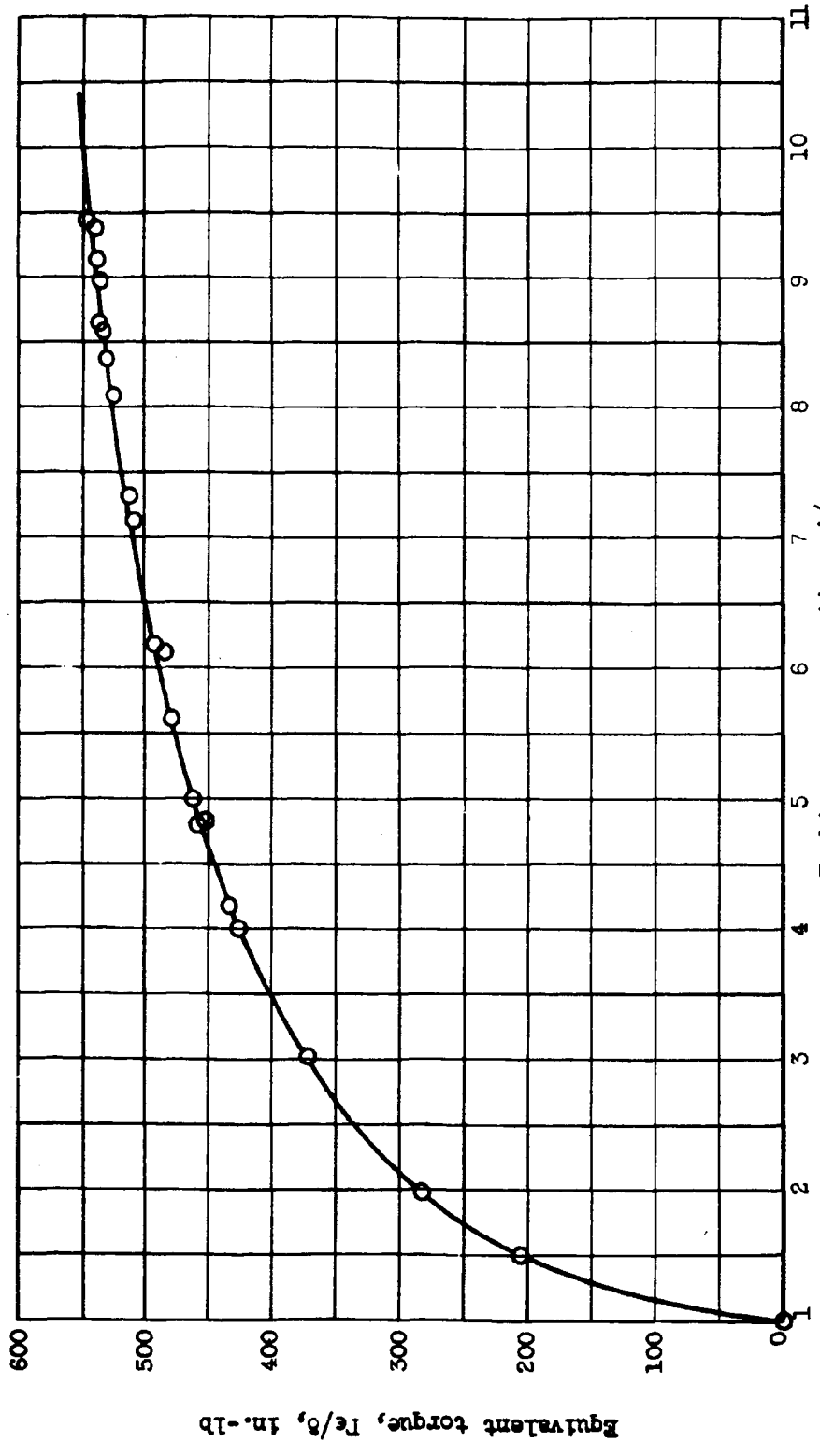

Figure 11. - Zero-speed turbine torque.

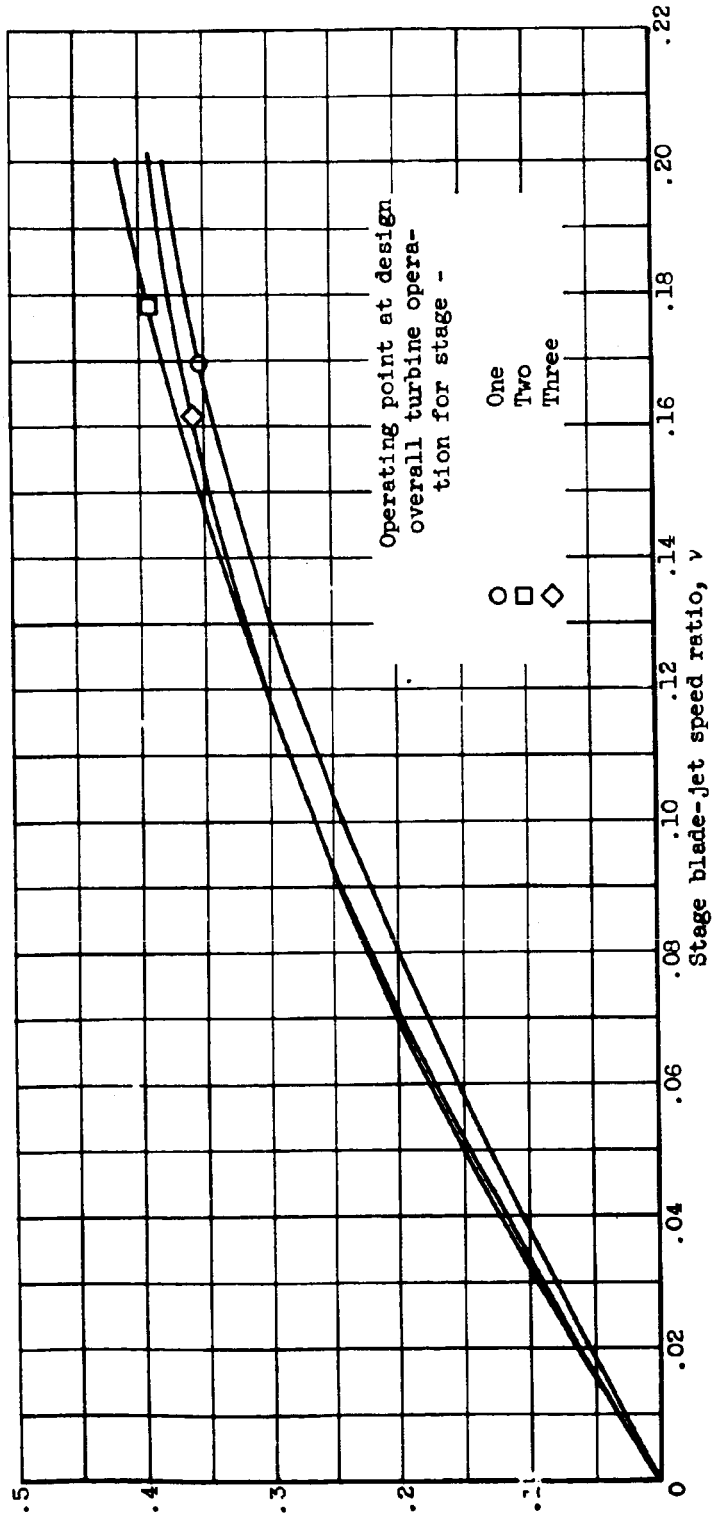

Figure 12. - Static efficiency adjusted for calculated inlet losses incurred during tests of the second and third stages.

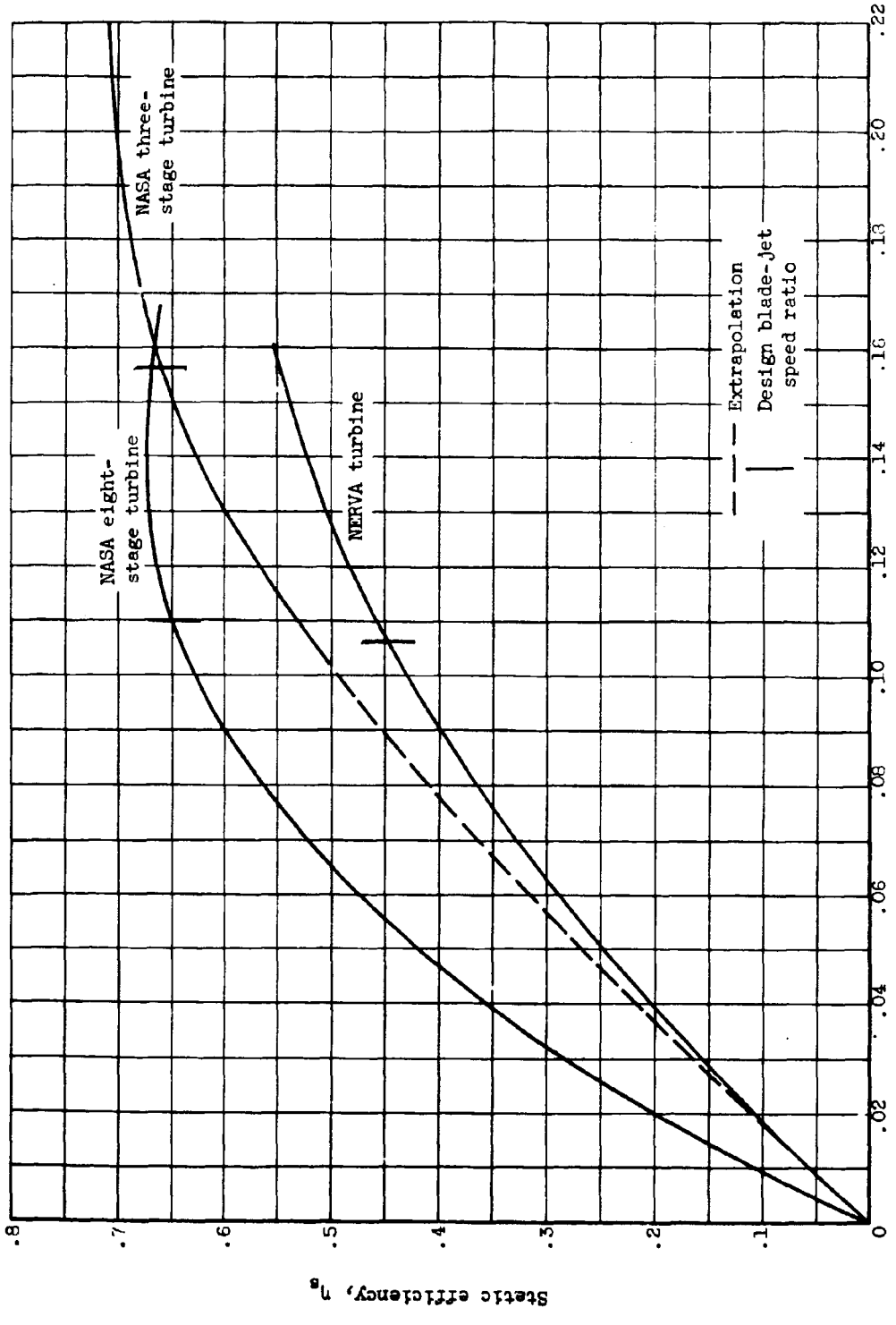

Figure 13. - Experimental efficiencies of three multistage turbines designed for low blade-jet speed ratios.

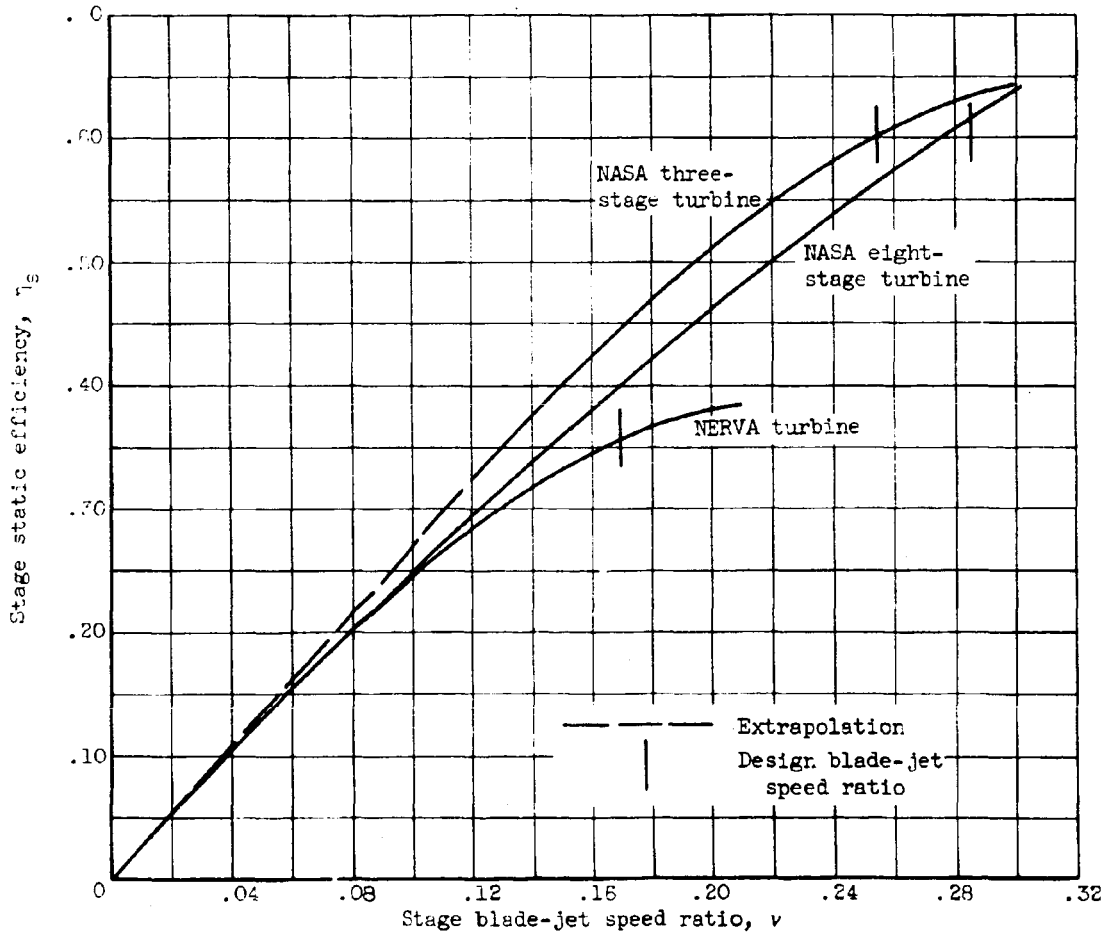

Figure 14. - First-stage efficiencies.